SOLUTION MINING RESEARCH INSTITUTE
679 Plank Road
Clifton Park, NY 12065, USA

Telephone: +1 518-579-6587
www.solutionmining.org

Technical Conference Paper

1965 – 2025

Parametric Study on the Effect of a Cavern's Aspect Ratio on Working Gas Capacity

Matt Jones, Maggie Sebert, and Josh Rath,
RESPEC, Rapid City, South Dakota, United States

SMRI Fall 2025 Technical Conference
29-30 September 2025
Wichita, Kansas, United States

Solution Mining Research Institute Fall 2025 Technical Conference

Wichita, Kansas, United States 29-30 September 2025

PARAMETRIC STUDY ON THE EFFECT OF A CAVERN'S ASPECT RATIO ON WORKING GAS CAPACITY

Matt Jones, Maggie Sebert, and Josh Rath

RESPEC, Rapid City, South Dakota, United States

Abstract

When developing new caverns for gas storage, the design must be based on the available space and planned operation requirements. Cavern size is determined by the desired storage volume, which is often constrained by surface area at a facility and geomechanical considerations. A cavern design with a high aspect ratio (i.e., high cavern height-to-diameter ratio) maximizes the volume for gas storage within a given facility property. The operational envelope of tall gas storage caverns, however, is often limited by the minimum gas pressure required to maintain cavern stability. Tall caverns also experience higher creep closure rates compared to shorter caverns of equivalent volume. These effects are often caused by increasing in situ temperatures and stresses with depth. Increased shear stresses around caverns at deeper depths are caused by the pressure differences within the cavern and the surrounding salt. Increased temperature at deeper depths increases the creep rate of the salt, as the salt creep rate is highly temperature dependent. These factors lead to increased minimum pressures required to mitigate closure and maintain the integrity of the salt on the cavern surfaces for taller, deeper caverns.

This parametric study sought to investigate the effect of a cavern's aspect ratio on its working gas capacity during the cavern's operational service life. Numerical models were used to simulate the solution mining, dewatering, and annual gas storage operations of hypothetical cavern designs with various aspect ratios to estimate the working gas capacity over time. The findings from this parametric study can be used to inform gas storage cavern designs and maximize the working gas capacity for the desired operational service life.

Key words: Caverns for Gas Storage, Cavern Design, Computer Modeling, Storage Capacity, Cavern Design Parameters, Aspect Ratio, Cavern Height, Cavern Radius, Cavern Diameter

Introduction

Cavern design for gas storage can impact the performance and lifespan of a gas storage cavern in domal salt formations. The capacity of a natural gas storage cavern is influenced by several factors, such as casing shoe depth, roof depth, cavern height, and cavern diameter. The depth of the casing shoe determines the allowable pressure conditions in gas storage caverns, as these conditions are typically limited by the pressure at the casing shoe, which depends on its depth. Although deeper casing shoe depths allow for higher maximum pressures in the cavern, the pressure gradient at the casing shoe remains unchanged. As a result, while the operating envelope is still constrained by the casing shoe gradient, deeper caverns can support higher operating pressures, which may translate into increased working gas capacity. Despite deeper caverns having higher pressure conditions than shallower ones, they are more susceptible to closure due to elevated temperatures and increased salt creep rate as well as increased in situ stresses and greater shear stresses around the cavern.

Additionally, because of the relatively low density of natural gas, the pressure difference between the casing shoe and the bottom of the cavern is small. This becomes increasingly evident with increased cavern height. Even at high-pressure conditions, the pressure in the bottom depths of the cavern is relatively low in

comparison to the in situ stress, which can result in increased shear stress in the salt around the lower portions of the cavern. In some cases, a cavern cannot be fully dewatered without exceeding the maximum allowable pressure gradient at the casing shoe depth, established to avoid fracturing the salt and exceeding in situ stresses at the casing shoe depth.

Increased cavern closure, additional shear stress in the salt around the cavern surfaces, and potential limitations on dewatering depth within established casing shoe pressure gradient limits are all potential challenges of developing very tall and deep gas caverns. Other challenges are possible when developing caverns with large diameters. Caverns with large diameters increase the potential for casing strain as the salt creeping downward at the cavern roof pulls the casing with it. These caverns also have a larger footprint from a plan-view perspective in cases where the surface area of a facility may be limited.

Given the mentioned factors to consider in a cavern design, this study investigated various cavern designs by assessing the gas storage capacity and geomechanical performance of caverns with different aspect ratios (cavern height-to-diameter ratio). To explore the impact of cavern aspect ratio on gas storage capacity and geomechanical performance, this study conducted a series of numerical simulations across a range of cavern designs. These simulations systematically varied cavern height, diameter, and depth to evaluate how different aspect ratios influence key performance indicators such as cavern closure, storage capacity, gas storage operating pressure limitations, and casing strain. By isolating and combining different geometric parameters, the study provides insight into the trade-offs and constraints associated with designing tall, wide, or deep caverns for gas storage in domal salt formations.

Technical Approach

To understand the effects of varying cavern aspect ratios, simple axisymmetric models were developed to estimate cavern storage capacity over a 10-year time period. Each model included a single cavern design within flat, uniform material layers of sediments, caprock, and salt. Each cavern model was represented as an axisymmetric, cylindrical geometry with arched edges at the roof and floor to avoid stress concentrations. The modeled stratigraphy and an example of one of the finite element meshes developed for the study are provided in Figure 1.

The elastic material properties of the overlying sediments were assumed to similar to those typical of shallow sediments found in the Gulf Coast. The elastic material properties of the caprock were assumed based on the typical properties for anhydrite. The densities, elastic material properties, and the modeled top of formation depths are listed in Table 1. To model the creep behavior of salt, the multimechanism deformation (M-D) creep model was used. This creep model captures the temperature dependency of salt creep rate, as well as transient, steady-state, work-hardening, and recovery stages of salt creep. The M-D parameter values used for this study correspond to soft salt, as defined by Munson [1998].

The in situ stress distribution within the salt was assumed to be isotropic (i.e., the horizontal stresses are equal to the vertical stress) for this study. The in situ stress state in salt formations is generally accepted to be nearly isotropic because salt creep tends to relieve large shear stresses over time. An accurate estimate of the in situ temperature and in situ stress are important when modeling salt creep because salt's creep rate is highly temperature dependent. The assumed in situ temperature profile is described in Equation 1 and is based on in situ temperature gradients typical of the Gulf Coast salt domes, assuming a surface temperature of 90 degrees Fahrenheit (°F).

$$90\ °F + 0.01\ °F/ft * depth \quad (32\ °C + 0.017\ °C/m * depth) \tag{1}$$

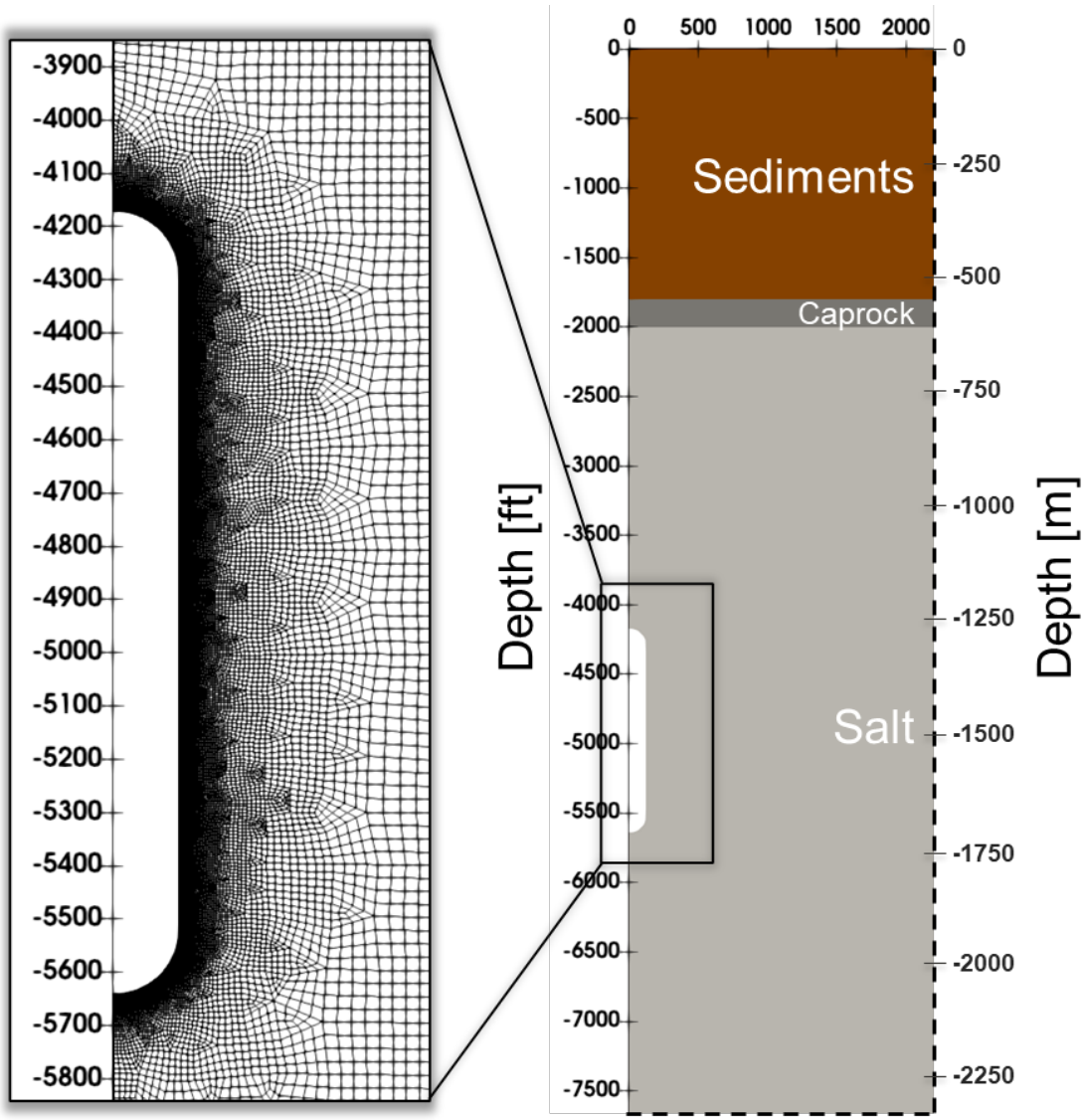

Figure 1. Example Cavern Mesh and Model Stratigraphy.

Table 1. Density, Elastic Material Properties, and Formation Top Depths.

Unit	Density		Young's Modulus		Poisson's Ratio	Formation Top Depth	
	pcf	kg/m^3	10^6 psi	GPa	—	ft	m
Sediments	125.8	2015	0.32	0.015	0.35	0	0
Caprock	184.8	2960	1339	64.1	0.34	1,800	548.6
Salt	135.5	2170	647	31.0	0.25	2,000	609.6

pcf = pounds per cubic foot
kg/m^3 = kilograms per cubic meter
GPa =gigapascal
ft = feet
m = meter

Axisymmetric Model Parameters

Table 2 lists the models and their corresponding cavern design parameters. In all models, the cavern roof was assumed to be 250 ft (76.2 m) below the casing shoe depth. The modeled cavern aspect ratios ranged between 1 and 12, with the following model sets assessed:

1. **Fixed Diameter:** Fixed diameter, fixed casing shoe depth, variable cavern volume
2. **Fixed Volume and Casing Shoe Depth:** Variable diameter, fixed casing shoe depth, fixed cavern volume
3. **Fixed Volume and Cavern Mid-Height:** Variable diameter, variable casing shoe depth, fixed cavern volume

The modeled cavern profiles for each of these cavern designs are depicted in Figure 2.

Table 2. Modeled Cavern Parameters.

Model Set	Aspect Ratio	Height		Diameter		Cavern Volume		Casing Shoe Depth	
		ft	m	ft	m	MMbbls	10^6 m^3	ft	m
1	1	200	61	200	61	0.746	0.119	3,500	1,067
	2	400	122			1.865	0.297		
	4	600	183			4.103	0.652		
	6	800	244			6.341	1.008		
	8	1,200	366			8.580	1.364		
	10	1,600	488			10.818	1.720		
	12	2,000	610			13.056	2.076		
2	1	500	152	500	152	11.657	1.853	3,500	1,067
	2	737	225	368	112				
	4	1,133	345	283	86				
	6	1,470	448	245	75				
	8	1,772	540	222	68				
	10	2,050	625	205	62				
	12	2,311	704	193	59				
3	1	500	152	500	152	11.657	1.853	4,400	1,341
	2	737	225	368	112			4,282	1,305
	4	1,133	345	283	86			4,083	1,245
	6	1,470	448	245	75			3,915	1,193
	8	1,772	540	222	68			3,764	1,147
	10	2,050	625	205	62			3,625	1,105
	12	2,311	704	193	59			3,494	1,065

m^3 = cubic meter
MMbbls = million barrels

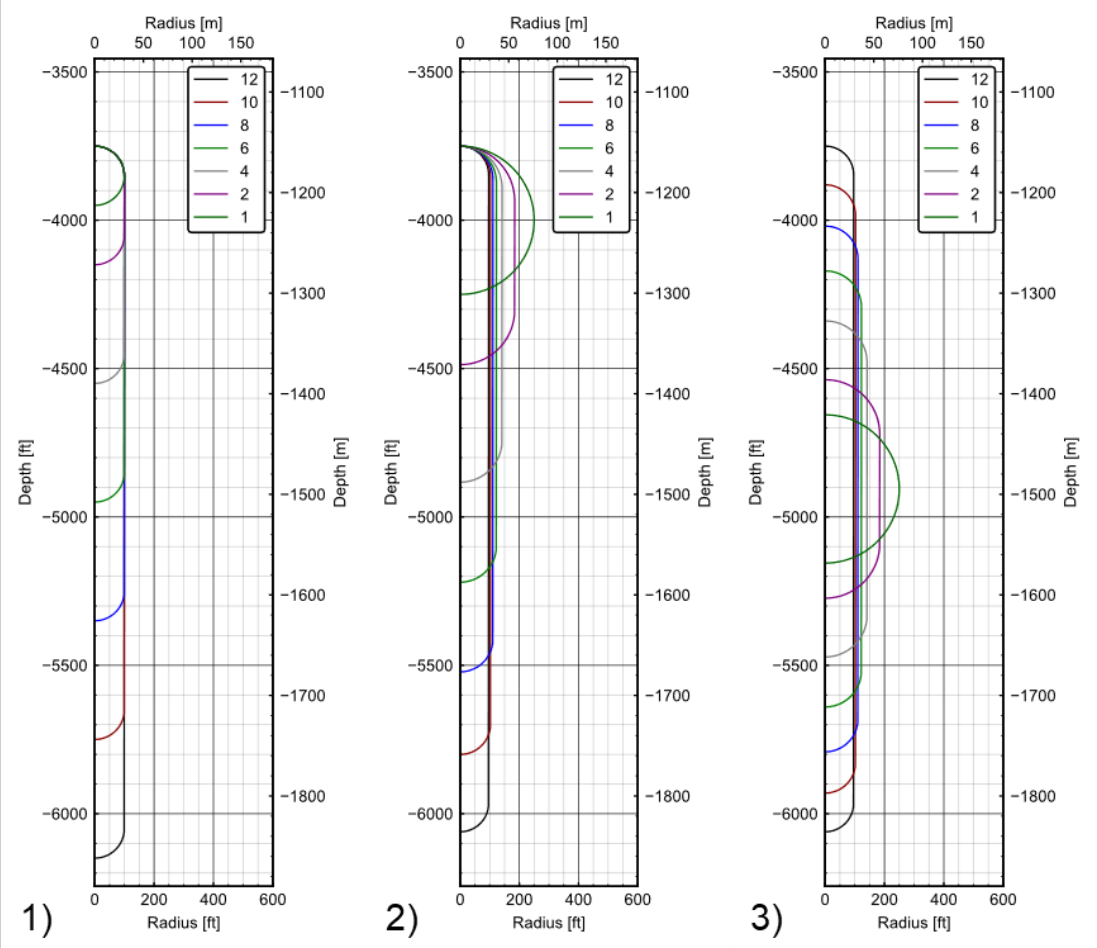

Figure 2. Axisymmetric Cavern Designs Modeled: (1) Fixed Diameter, (2) Fixed Volume and Casing Shoe Depth, and (3) Fixed Volume and Cavern Mid-Height.

Gas Storage Operations Simulated

Solution mining, dewatering, gas drawdown, and 10 years of gas operations were simulated for each model set described in the Axisymmetric Model Parameters Section. The solution mining durations were individualized based on a constant flow rate of fresh water throughout injection and the volume of salt assumed to have been solution mined. After solution mining, the dewatering durations were also scaled based on the modeled cavern volume. At the end of dewatering, all caverns were held at high pressure for 60 days before an annual gas storage operation cycle was modeled for 10 years.

Table 3 provides the assumed composition for the natural gas stored in the caverns. The modeled annual gas storage operation cycle was generic and defined by RESPEC in terms of inventory percentage based on typical cavern operations in the Gulf Coast region [Vining, C. and K. L. DeVries, 2011]. Figure 3 illustrates the annual gas storage cycle, in terms of product inventory percentage, repeated in all the models.

In the annual gas storage operation cycle, a 100 percent inventory was assumed when the cavern was at its maximum allowable operating pressure. For this study, the maximum allowable operating pressure was assumed to be at the casing shoe gradient of 0.9 pound per square inch per foot (psi/ft) (20.4 Kilopascal per meter [kPa/m]). The cavern was assumed to have 0 percent inventory when at its minimum allowable operating pressure.

Table 3. Natural Gas Composition Modeled.

Gas Component	Mole Percent
Methane	93.34
Nitrogen	1.71
Carbon Dioxide	0.64
Ethane	3.40
Propane	0.63
i-Butane	0.08
n-Butane	0.10
i-Pentane	0.06
Helium	0.04

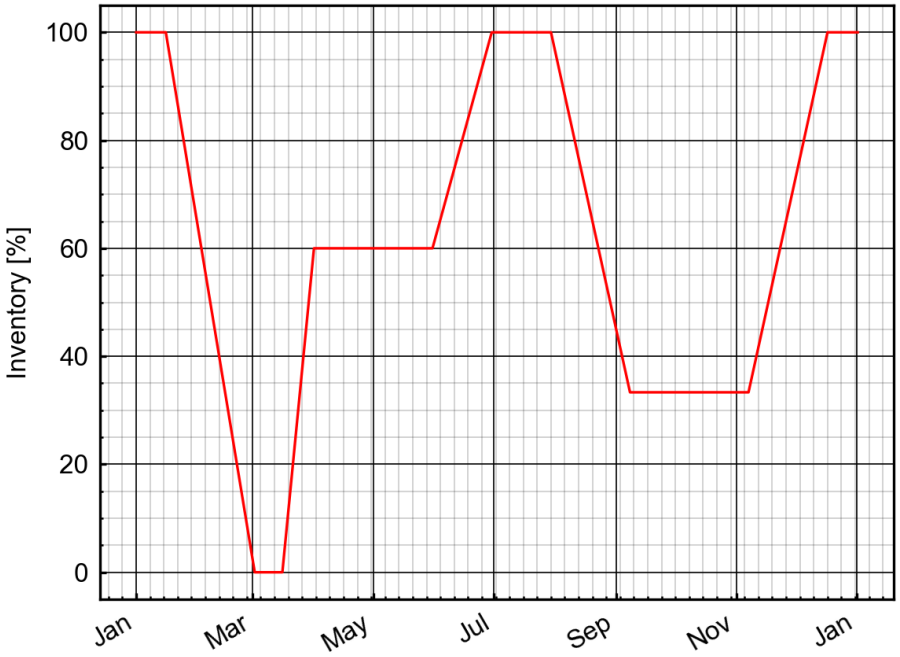

Figure 3. Modeled Annual Gas Storage Operation Cycle Relative to Individual Cavern Gas Inventory.

An appropriate minimum pressure was determined for each cavern by limiting the salt volume predicted to be in a dilatant state during a 45-day gas withdrawal simulation. This gas withdrawal was simulated after the caverns' development, dewatering, and quiescent period (i.e., holding the cavern at high pressure for 60 days). The withdrawal simulation began at the maximum casing shoe pressure gradient of 0.9 psi/ft (20.4 kPa/m) and was continuously lowered to 0.2 psi/ft (4.52 kPa/m). Dilation factors of safety in the salt were evaluated as the cavern was depressurized to establish a relationship between cavern pressure and salt damage. Based on these results, the minimum allowable casing shoe pressures were established by determining the casing shoe gradient when the volume of salt predicted to dilate around the cavern was 1 percent of the cavern volume. After determining the minimum allowable casing shoe gradients, a 10-year gas storage operation was simulated. Figure 4 provides a visual representation of the cavern development and gas operation timeline simulated for each cavern across all model sets.

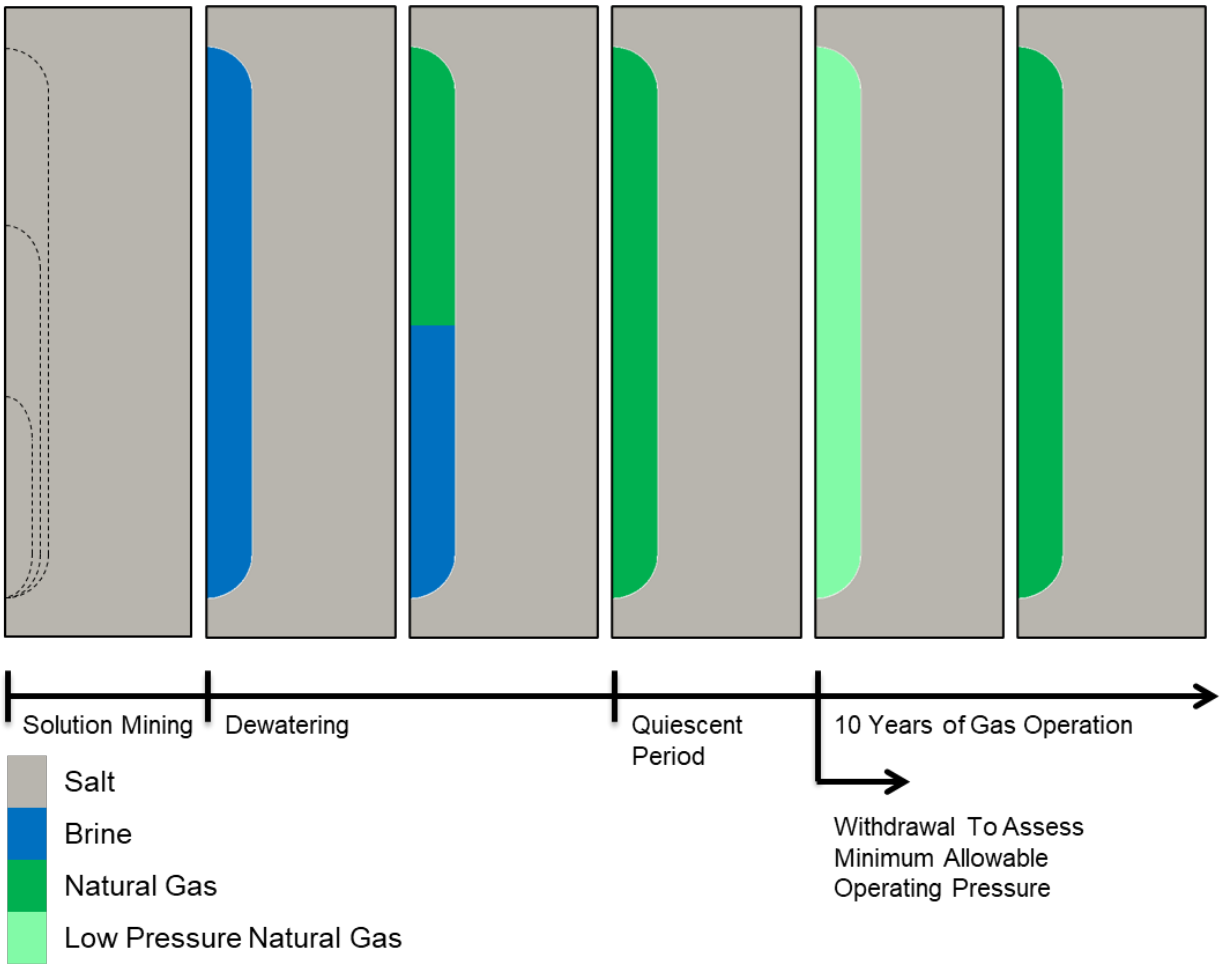

Figure 4. Diagram of the Simulated Cavern Development and Gas Operation Timeline.

Modeling Workflow and Tools

Salt Cavern Thermal Simulator (SCTS) [Nieland, 2004], in combination with SPECTROM-32 (SPE-32) [Callahan et al., 1989], was used to simulate the development and operation of the cavern designs in this study. SCTS is a program that simulates thermodynamics and heat transfer related to gas storage in underground salt caverns. This program accounts for the thermal effects associated with gas compression and expansion, mass transfer during injection and withdrawal, and heat transfer between the gas and its surroundings in the wellbore and cavern. SPE-32 is a finite element program developed by RESPEC to solve rock-mechanics problems, specifically to simulate underground openings and structures. This program can model the elastic-plastic response commonly associated with brittle rock types as well as simulate the viscoplastic behavior observed in rock salt. The following steps were taken to simulate the development and operation of the cavern designs using SCTS and SPE-32:

1. Solution Mining
    a. (SCTS) Estimate temperature field surrounding cavern from its development
    b. (SPE-32) Model mechanical and viscoplastic response of salt surrounding the cavern using brine column as pressure traction on the cavern surface
2. Dewatering and Quiescent Period
    a. (SCTS) Estimate gas pressure and density throughout dewatering

   b. (SPE-32) Model mechanical and viscoplastic response of salt surrounding cavern using moving gas/brine interface and gas pressure and density as pressure tractions on the cavern surface to simulate dewatering
3. Gas Withdrawal to Assess Minimum Allowable Operating Pressure
   a. (SCTS) Estimate gas pressure and density through withdrawal
   b. (SPE-32) Model mechanical and viscoplastic response of salt surrounding the cavern using gas pressure and density as pressure tractions on the cavern surface to determine minimum allowable operating pressure to limit dilation
4. 10 Years of Gas Storage Operations
   a. (SCTS) Estimate gas flow rates, pressure, and density throughout gas storage operations
   b. (SPE-32) Model mechanical and viscoplastic response of salt surrounding the cavern using gas pressure and density as pressure tractions on the cavern surface
   c. (SCTS) Estimate gas flow rates, pressure, and density throughout gas storage operations, including closure determined in SPE-32 to estimate base and working gas volume throughout storage operations

Evaluation Criteria

The following criteria were used in post-analyses of the numerical modeling results to assess the minimum allowable gas pressures and working gas capacity. These criteria were also used to examine the potential for cavern creep closure to cause damage to the cemented production casings in the wells.

Minimum Allowable Operating Pressure

Rock salt is a viscoplastic material that does not typically experience brittle failure under the loading conditions expected around solution-mined caverns, which is one of the reasons salt is a favored storage medium. The gas pressure in a cavern helps support the geological loads acting on the rock salt surrounding the cavern. As the gas pressure decreases, the loads that must be supported by the surrounding salt increase, which increases the potential for dilation in the salt surrounding the cavern. Dilation is the volumetric expansion of the salt resulting from microfracturing along the salt grain boundaries and is often referred to as salt damage. Salt damage is a progressive process whose severity will increase and accumulate as long as the shear stress exceeds the strength of the salt. If dilating states of stress are maintained for extended periods or are induced frequently because the gas pressure is low, the resultant microfracturing can coalesce and slabs of salt can spall from the cavern roof and walls. Therefore, cavern structural stability is maintained by operating the cavern at pressures greater than the recommended minimum to avoid or limit microfracturing (i.e., dilation) of the salt on the cavern surface.

A rapid, continuous gas withdrawal is believed to be the worst-case scenario for causing salt dilation because the time available for the salt to redistribute the increased loading through creep deformation is minimal. With time, salt creep will redistribute the increased loading farther from the cavern walls, reducing the shear stress and subsequently reducing the potential for dilating the salt near the cavern surface. During rapid gas withdrawal from a cavern, the salt is typically predicted to begin dilating in areas of stress concentration, such as sharp corners in the cavern wall. As the gas pressure continues to decrease, the salt over the entire surface of the cavern can begin to dilate. To avoid salt spalling from the cavern walls and roof, a minimum allowable gas pressure can be determined that precludes a significant amount of salt dilation around the cavern.

The recommended minimum allowable gas pressure is typically the pressure during a simulated withdrawal at which the volume of dilating salt is predicted to be 1 percent of the cavern volume (i.e., the normalized dilating salt volume). This approach was used to establish a minimum pressure for the gas operations simulated in this study. By illustrating the salt dilation factor-of-safety contours with a decreasing casing shoe gradient during gas withdrawal, Figure 5 shows salt dilation when establishing the cavern's minimum casing shoe pressure. In this study, factors of safety against damage potential were as described in Van Sambeek et al. [1993] and in Equation 2. Salt dilation factor-of-safety values less than 1.0 indicate regions of salt that are predicted to be in a dilatant state of stress.

$$\sqrt{J_{2,dil}} = 0.18 \cdot I_1 \quad (2)$$

where: $J_2 = \frac{1}{6} \cdot ((\sigma_1 - \sigma_2)^2 + (\sigma_2 - \sigma_3)^2 + (\sigma_3 - \sigma_1)^2)$

$I_1 = \sigma_1 + \sigma_2 + \sigma_3$

J_2 is the second invariant of the deviatoric stress tensor at the onset of dilation. I_1 is the first invariant of the stress tensor and is equal to three times the mean stress.

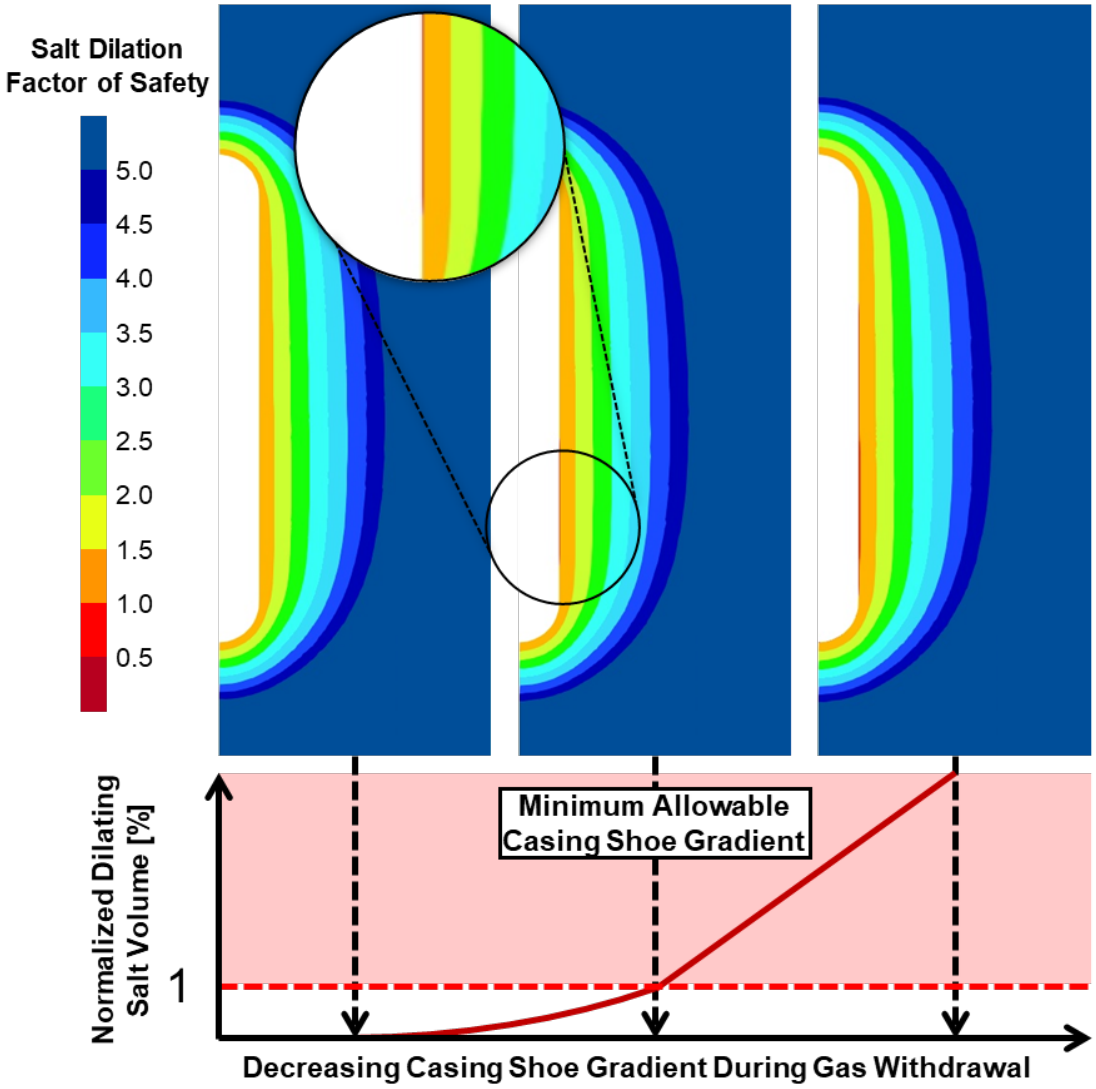

Figure 5. Diagram of Minimum Allowable Casing Shoe Gradient Determination Based on 1 Percent Normalized Dilating Salt Volume.

Working Gas Capacity

The working gas capacity was calculated by taking the difference between the total gas volume and the required base gas volume. The total gas volume is the gas volume when a cavern is at its maximum pressure, and the base gas volume is the gas volume when a cavern is at its minimum pressure. The working gas capacity was calculated over the 10 years of simulated gas operations and accounted for the

change in cavern volume from estimated cavern closure. The base and working gas volumes were compared at the end of the 10-year simulated gas operations. Storage efficiency was also assessed by calculating the percentage of the working gas volume to the total gas volume. The greater the storage efficiency, the less base gas volume must be left in the cavern to maintain the minimum allowable casing shoe gradient relative to the cavern's total gas volume, and the more effectively the cavern volume is used for gas storage.

Potential for Casing Damage

The creep behavior of salt causes caverns to gradually close and decrease in volume. When salt creeps into a cavern, it drags along the cavern's cemented casing, typically resulting in extensional axial strains in the casing. With time, these axial strains increase because salt creep continues to pull on the casing. If the tensile strength of the casing or casing connections is exceeded, the casing may be damaged and lose hydraulic integrity. Previous evaluations performed by RESPEC (e.g., Osnes et al. [2007]) indicated that cemented casings, with a variety of completions, have failed at the casing connections when the predicted axial strain exceeded 3.2 millistrain; therefore, a strain limit of 3.2 millistrain was used in this study. This criterion assumes that the casing is perfectly bonded to the cement, which is perfectly bonded to the rock strata. This approach is conservative because it ignores any slip between the casing and the rock strata that would relieve stress. Casing damage potential was also evaluated by comparing the predicted vertical strains along the path of the casings to a strain value of 3.2 millistrain.

Results

For each modeled cavern design, the cavern performance quantities were estimated, including closure, minimum allowable pressure, base gas volume, working gas volume, storage efficiency, and casing strain. These quantities were compared to one another to assess the influence of each cavern's aspect ratio on working gas volume and storage performance.

Cavern Closure

When salt creep relieves shear stress within the salt surrounding a cavern, the cavern volume decreases (closes) over time. This phenomenon leads to a loss in storage capacity throughout the lifespan of a cavern. Salt creep rate is highly temperature dependent, creeping faster with increased temperatures. Increased in situ temperatures, differences between in situ stress and cavern pressure, and, thus, increased creep rates are predicted to increase with depth. Therefore, salt toward the cavern bottom is more subject to creep-induced closure, which is increasingly evident for taller cavern designs.

The total cavern closures for all of the modeled caverns after 10 years of gas storage operations are provided in Figure 6. The caverns with the highest aspect ratio of 12 (the tallest caverns) are predicted to experience the most closure, which is expected because the taller the cavern, the higher the temperature conditions and stress differences it is subject to. Within the Fixed Diameter model set, the total cavern closure increased by 188 percent across aspect ratios of 1 to 12. This is due to the increase in cavern volume with increasing aspect ratio. Within the Fixed Volume model sets, the caverns with the highest aspect ratios experienced the largest total closure. For the Fixed Volume and Casing Shoe model set, the total closure between aspect ratios of 1 to 12 increased by 139 percent. Likewise, the Fixed Volume and Cavern Mid-Height model set had the highest closure among all aspect ratios, with an increase of 45 between aspect ratios of 12 to 1. This is because they are deeper than their direct comparisons and, therefore, subject to higher in situ temperatures, in situ stresses, and increased salt creep rates.

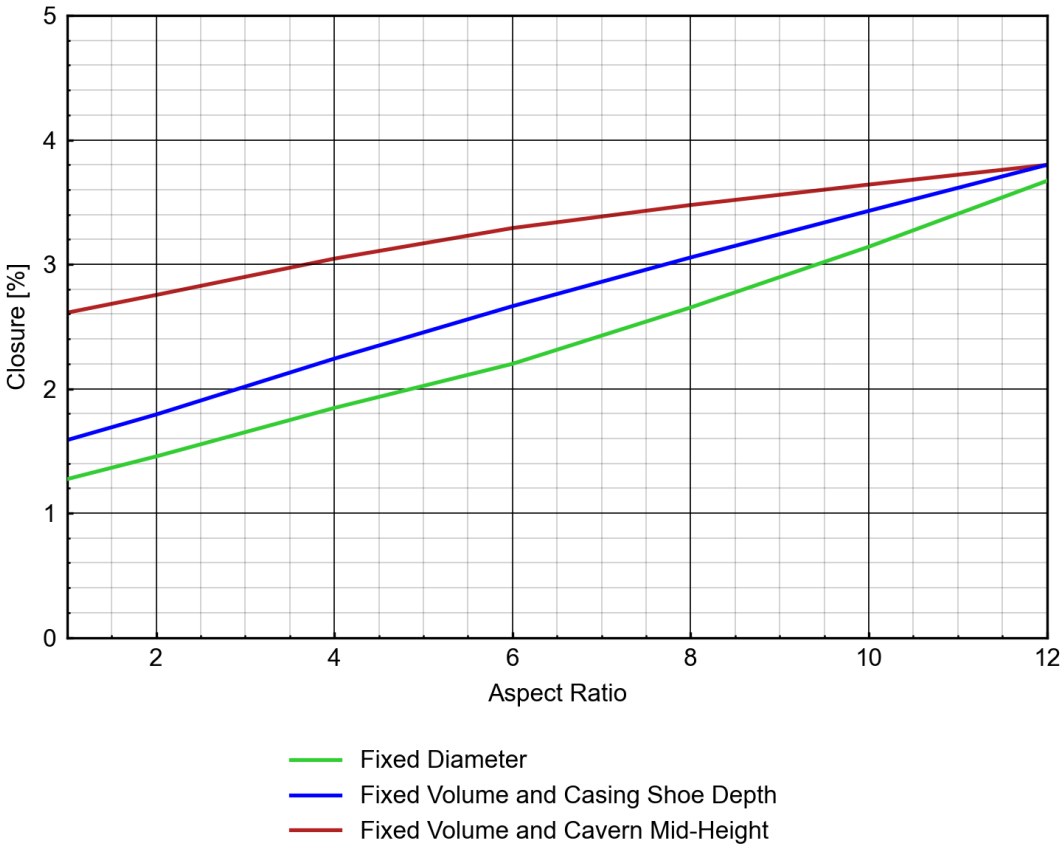

Figure 6. Cavern Closure Induced by Creep After 10 Years of Gas Storage Operations.

Minimum Pressure Requirements

A minimum allowable operation pressure was determined for each of the modeled cavern designs, which was set based on limiting salt dilation. Figure 7 shows the determined minimum allowable operating pressure for each cavern design within each model set as a function of aspect ratio. Overall, higher minimum pressure conditions are predicted for increased cavern height-to-diameter aspect ratios. These results are caused by increased cavern height and, therefore, increased stress differences over the cavern height and around the lower depths of the cavern interval. Minimum pressure increased by 53 percent between the aspect ratios of 12 and 1 within the Fixed Diameter model set. Within the Fixed Volume and Casing Shoe Depth model set, the minimum pressure increased by 53 percent, and by 64 percent within the Fixed Volume and Cavern Mid-Height model set. The differences in minimum pressure between the model sets are likely caused by the variation in casing shoe depth, as the Fixed Volume and Cavern Mid-Height model set included deeper casing shoe depths than those of the Fixed Volume and Casing Shoe Depth model set and Fixed Diameter model set.

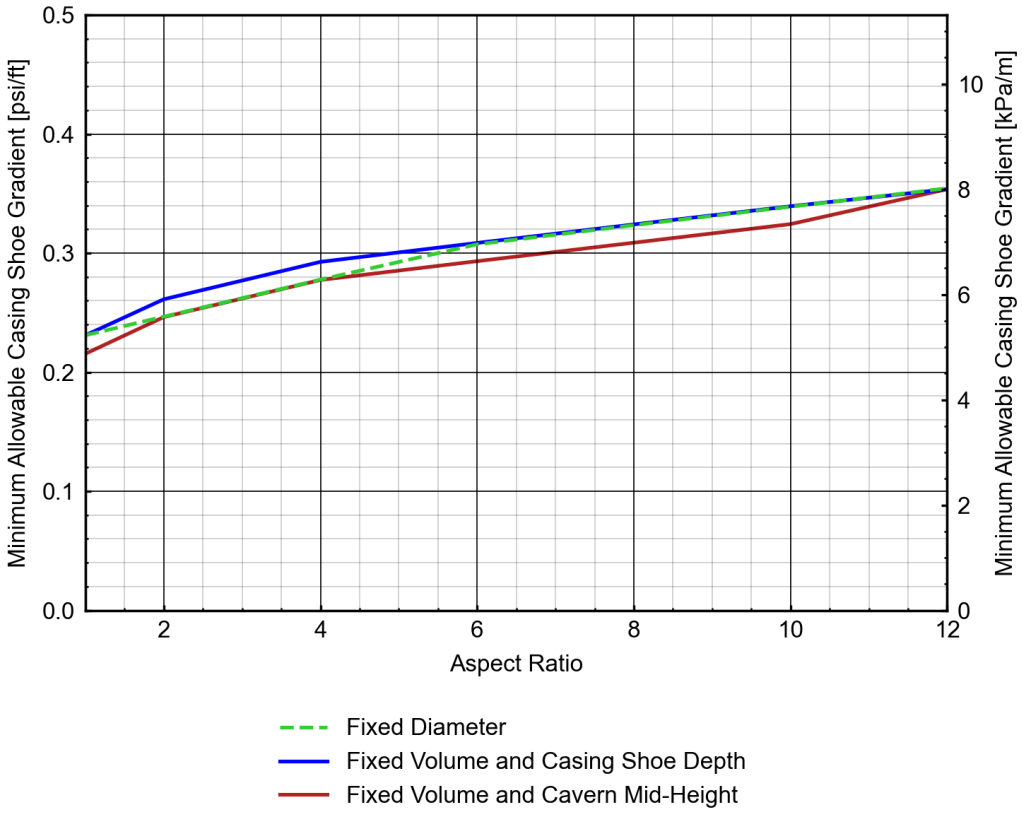

Figure 7. Minimum Allowable Operating Pressure Versus Aspect Ratio.

Base Gas Requirements

A minimum volume of gas (i.e., base gas volume) must remain in the cavern to maintain cavern stability and limit salt dilation. In most cavern storage operations, base gas volume is undesirable because it cannot be used during normal operations and can only be retrieved by rewatering the caverns. The base gas for each cavern design set was estimated by determining the gas volume at the minimum pressure during gas operation and plotting it versus the aspect ratio, as depicted in Figure 8.

For the Fixed Diameter model set, the required base gas volume increased with aspect ratio. In this model set, increasing the aspect ratio from 1 to 12 increased the volume by 1,700 percent and the required base gas by 2,700 percent. In other words, there is a nonlinear relationship between cavern volume/height and the required base gas if the diameter of a cavern is fixed. This nonlinearity is because of the increase in minimum pressure and therefore the increase in base gas volume, as cavern height is increased.

The required base gas volume increased as the aspect ratio increased in the Fixed Volume model sets, despite having equivalent cavern volumes. When the cavern volume and casing shoe depth were fixed, changing the aspect ratio from 1 to 12 increased the base gas volume by 45 percent. This result suggests that increasing the aspect ratio of the cavern increases the required base gas volume independently of cavern volume. When the cavern volume was fixed and the casing shoe depth became shallower with increasing cavern aspect ratio, the base gas increased by 22 percent. This result suggests that increasing the depth of the cavern also increases the required base gas volume, independent of aspect ratio and volume. Table 4 lists the base gas volumes required and percentage differences relative to the cavern design with an aspect ratio of 1, calculated for each aspect ratio between each modeled depth. This table also describes the percentage differences between the Fixed Volume model sets for each aspect ratio.

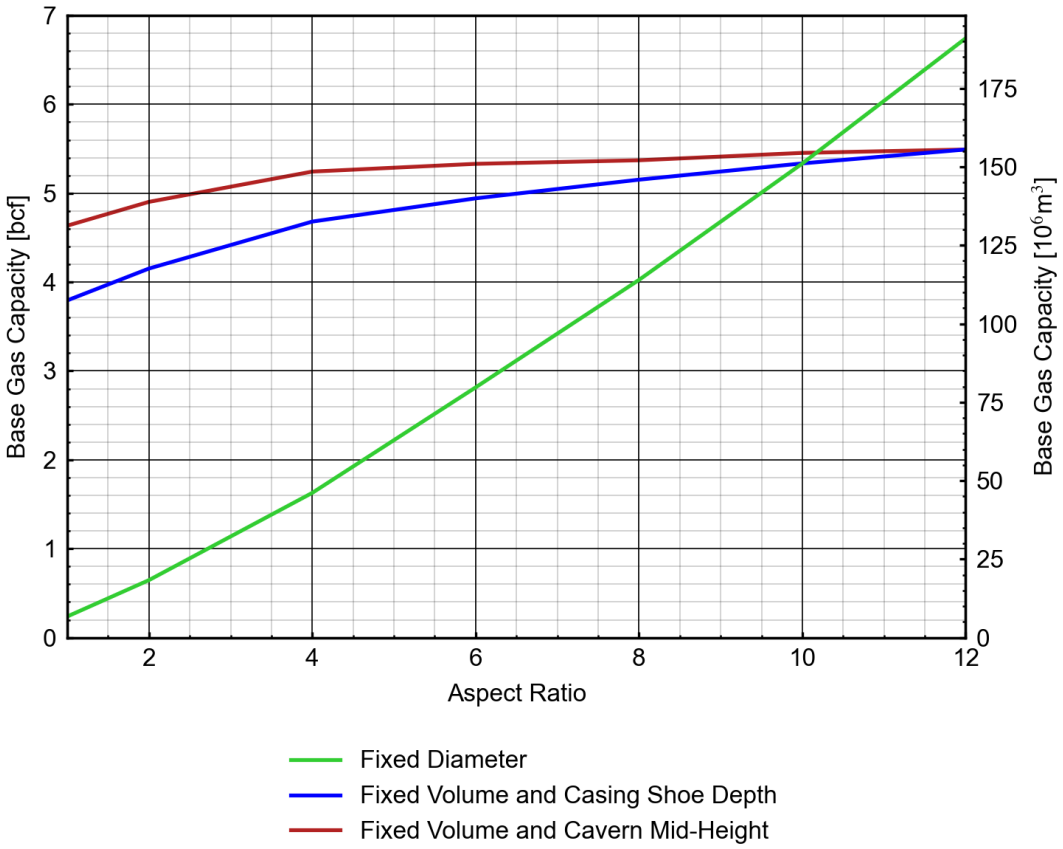

Figure 8. Base Gas Volume Required Versus Aspect Ratio After 10 Years of Gas Storage Operations.

Table 4. Base Gas Volume Required and Percent Difference After 10 Years of Gas Storage Operations for Fixed Volume Cavern Designs.

Aspect Ratio	Fixed Casing Shoe Depth			Variable Casing Shoe Depth			Percent Difference Between Model Sets %
	Base Gas Required		Percent Difference %	Base Gas Required		Percent Difference %	
	bcf	10^6 m^3		bcf	10^6 m^3		
1	3.8[(a)]	107[(a)]	0.0	4.6[(a)]	131[(a)]	0.0	22.2
2	4.2	118	9.5	4.9	139	5.8	18.1
4	4.7	133	23.4	5.2	148	13.1	12.0
6	4.9	140	30.3	5.3	151	15.0	7.9
8	5.2	146	35.8	5.4	152	15.9	4.2
10	5.3	151	40.6	5.5	154	17.7	2.2
12	5.5	156	44.8	5.5	156	18.5	0.0

(a) The percent difference was calculated for each aspect ratio and casing shoe depth iteration relative to this value.

Working Gas Capacity

The working gas capacity is the volume of natural gas available to be withdrawn from the cavern throughout normal operations and is defined as the difference between the total gas capacity and required base gas. As caverns increase in total volume, their total gas capacity also increases. However, the base gas requirement and the amount of gas in a cavern that cannot be withdrawn also increase, resulting in a relationship between the cavern volume and working gas capacity that does not necessarily scale proportionally. Figure 9 presents the working gas capacity results for the different model sets as a function of aspect ratio. As anticipated, for the Fixed Diameter model set, working gas capacity increases with an increase in cavern volume, though not proportionally. This is because taller and deeper caverns require more base gas, which reduces overall storage efficiency. Upon the cavern volume being fixed, the working gas capacity decreases with increasing cavern aspect ratio because of the increased required base gas in taller and deeper caverns.

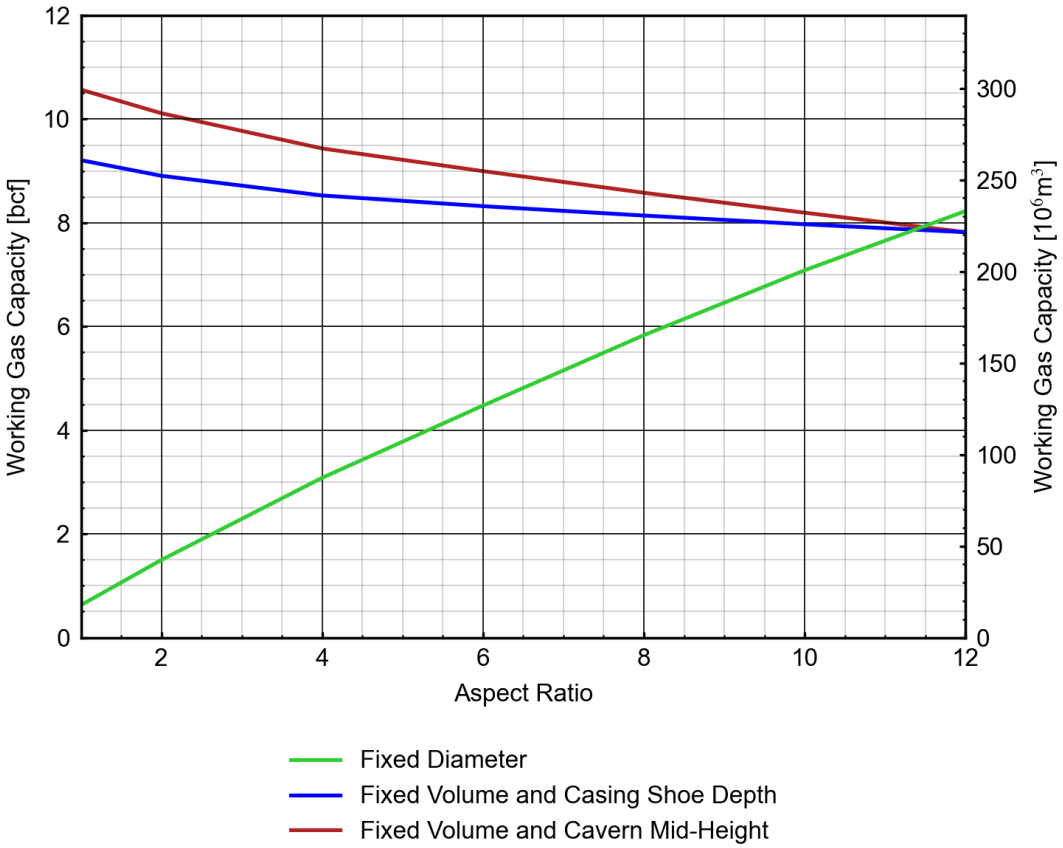

Figure 9. Working Gas Volume Versus Aspect Ratio After 10 Years of Gas Storage Operations.

In understanding the effects of various cavern depths on the working gas capacity, the two Fixed Volume model sets were compared, and the results are included in Table 5. For both sets of cavern designs, the percent difference in the working gas capacity relative to the cavern design with an aspect ratio of 1 was calculated. In both scenarios, there was a decrease in working gas capacity with increased aspect ratio. Additionally, the percentage difference between the model sets was calculated for each aspect ratio. In comparing the same cavern aspect ratios between the Fixed Volume model sets, a cavern of the same volume and design at a deeper depth has an increased working gas capacity, as long as the full volume can be dewatered. This is the case as the minimum pressure conditions in deeper caverns are higher than those of shallower caverns with the same design, decreasing the base gas volume.

Table 5. Working Gas Volume and Percent Difference After 10 Years of Gas Storage Operations for Fixed Volume Cavern Designs.

Aspect Ratio	Fixed Casing Shoe Depth			Variable Casing Shoe Depth			Percent Difference %
	Working Gas Capacity		Percent Difference %	Working Gas Capacity		Percent Difference %	
	bcf	10^6 m^3		bcf	10^6 m^3		
1	9.2[(a)]	261[(a)]	0	10.6[(a)]	299[(a)]	0	15
2	8.9	252	-3	10.1	286	-4	14
4	8.5	241	-7	9.4	267	-11	11
6	8.3	236	-10	9.0	255	-15	8
8	8.1	230	-12	8.6	243	-19	5
10	8.0	226	-13	8.2	232	-22	3
12	7.8	221	-15	7.8	221	-26	0

bcf = billion cubic feet

(a) The percent difference for each aspect ratio and casing shoe depth iteration was relative to the respective cavern design with an aspect ratio of 1.

Gas Storage Efficiency

After estimating the base and working gas volume for each of the cavern designs, gas storage efficiency was calculated by dividing the working gas volume by the total gas volume. In a cavern with 100 percent storage efficiency, all of the gas can be injected and withdrawn from the cavern. However, this is not achievable in salt caverns because a base gas volume is required to maintain cavern stability. Figure 10 presents the storage efficiency for each model set plotted against the aspect ratio. In all scenarios, the cavern designs became less efficient for gas storage with increased aspect ratios. The Fixed Volume and Cavern Mid-Height model set had the least chance in efficiency of the three scenarios.

In all model sets, the storage efficiency decreased with increased aspect ratios. The greatest loss experienced is in the Fixed Diameter model set, with a storage efficiency decrease of 18 percent, from 73 percent at an aspect ratio of 1 to 55 percent at an aspect ratio of 12. The Fixed Volume model sets indicate that storage efficiency is decreased as the cavern designs are deeper. This is because, although the working gas capacities for the cavern designs in the Fixed Volume and Cavern Mid-Height model set are the greatest, so are the base gas volumes.

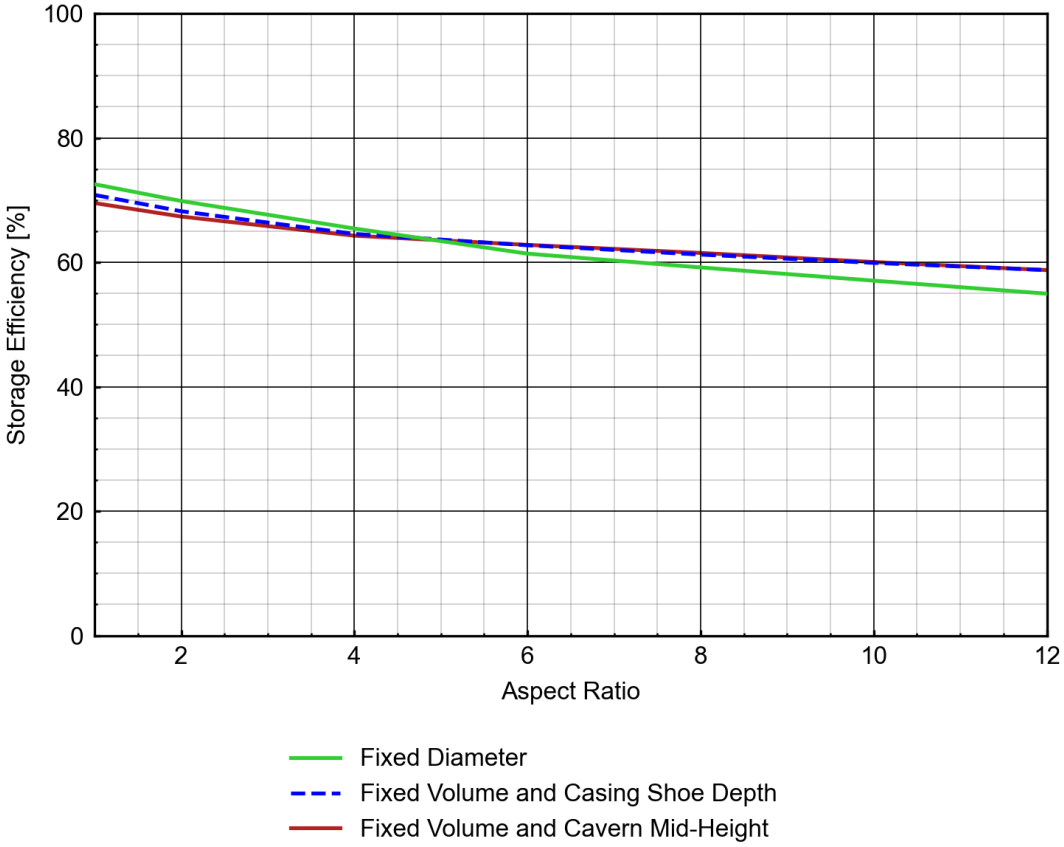

Figure 10. Storage Efficiency After 10 Years of Gas Storage Operations.

Potential for Casing Damage

Although maximizing working gas capacity and storage efficiency is a primary consideration for cavern designs, maintaining integrity within the cemented casing over the desired life of the cavern must be considered. As a cavern experiences creep closure, the cavern roof salt creeps downward and induces strain within the casing, which creates the potential for casing damage and hydraulic integrity loss. The predicted vertical strain at the casing shoe depth after 10 years of gas storage operation plotted against the cavern aspect ratio is illustrated in Figure 11.

In all model sets, the predicted casing strain after 10 years of gas storage operation is not predicted to exceed 3.2 millistrain, suggesting that under these conditions, casing damage is not predicted to occur in the modeled cavern designs. In the Fixed Volume and Cavern Mid-Height model set, increasing the aspect ratio from 1 to 12 decreased the casing strain at the casing shoe depth by 93 percent. The casing strain at the casing shoe depth predicted in the Fixed Volume and Casing Shoe Depth model set decreased by 87 percent as the aspect ratio increased from 1 to 12. The maximum predicted casing strain for the Fixed Volume model sets in the cavern designs with an aspect ratio of 1 was approximately 94 percent greater for that of the fixed cavern mid-height relative to the fixed casing shoe depth. Unlike the model sets with fixed volume, the casing strain predictions for the Fixed Diameter model set does not change significantly across the range of aspect ratios between 1 and 12.

The Fixed Volume model sets indicate that casing deformation is influenced by depth (cavern and casing shoe). This is caused by the increased creep rates as a result of higher temperatures and in situ stresses. The results from the Fixed Diameter model set suggest that varying cavern height, volume, and aspect ratio have a minimal effect on casing deformation. Instead, cavern diameter was the dominant factor.

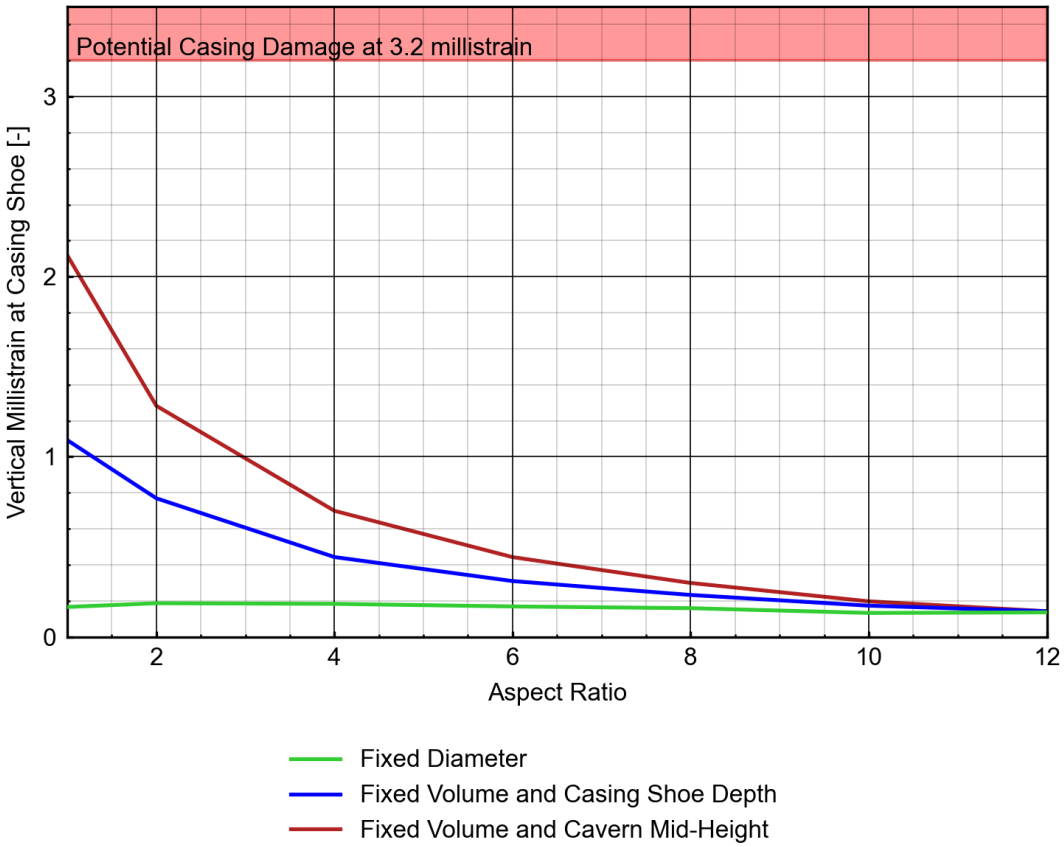

Figure 11. Vertical Strain at the Casing Shoe Depth as a Function of Aspect Ratio After 10 Years of Gas Storage Operations.

Rather than as a function of aspect ratio, casing strain as a function of cavern diameter for the three model sets was considered, and the results are shown in Figure 12. With increasing cavern diameter and, therefore, roof diameter, the total predicted casing strain increased. The cavern aspect ratio and depth have less of an effect on casing strain. The Fixed Volume and Cavern Mid-Height model set yielded higher predicted casing strain values than those of the Fixed Volume and Casing Shoe Depth model set. This result is because of increased temperature and, therefore, increased salt creep rate for the cavern models with deeper casing shoe depths. The Fixed Diameter model set indicated very little change in the predicted casing strain, indicating a minimal effect of the aspect ratio on the predicted casing strain values.

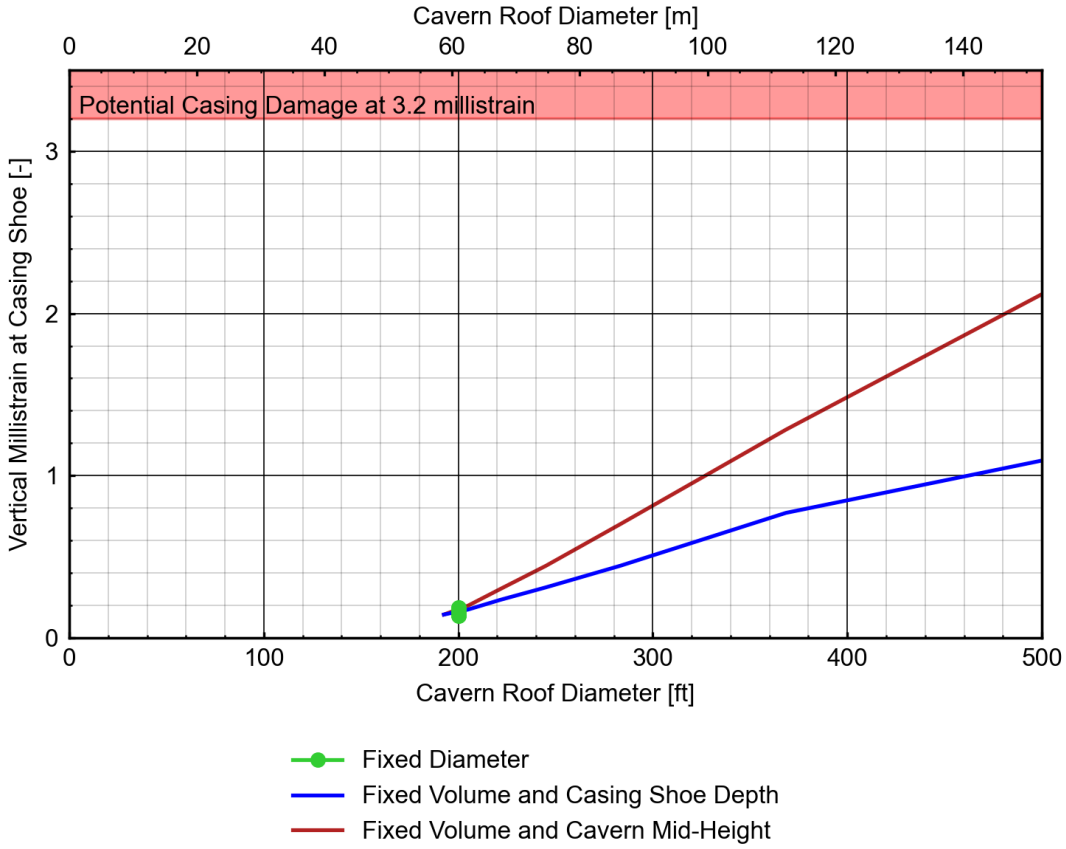

Figure 12. Vertical Strain at Casing Shoe Versus Cavern Roof Diameter After 10 Years of Gas Storage Operations.

Conclusions

This parametric study assessed the influence of cavern aspect ratio on working gas capacity using numerical simulations of an idealized gas storage cavern. The simulations included solution mining, dewatering, a gas drawdown, and 10 years of a generic annual natural gas storage cycle. The following three cavern design sets were analyzed with aspect ratios (height-to-diameter) of 1, 2, 4, 6, 8, 10, and 12:

- **Fixed Diameter:** Fixed diameter and casing shoe depth; variable volume.
- **Fixed Volume and Casing Shoe Depth:** Fixed volume and casing shoe depth; variable diameter.
- **Fixed Volume and Cavern Mid-Height:** Fixed volume and mid-height; variable diameter and casing shoe depth.

The following conclusions in terms of key considerations for gas cavern design were drawn from the numerical simulations performed for this study:

- **Cavern Closure:** Cavern closure increases with depth as a result of elevated shear stress and temperature, which accelerate salt creep. Designs spanning deeper intervals experience greater closure.
    - After 10 years of gas storage, cavern closure increased by 188, 139, and 45 percent between aspect ratios 1 and 12 for the Fixed Diameter model set, Fixed Volume and Casing Shoe Depth model set, and Fixed Volume and Cavern Mid-Height model set, respectively.

- **Minimum Pressure:** Higher aspect ratio caverns require greater minimum pressure to maintain stability and prevent salt dilation.
    - Minimum pressure increased by 53, 53, and 64 percent between aspect ratios 1 and 12 across the three model sets.
- **Base Gas Requirements:** Base gas volume needed to maintain minimum pressure and cavern stability increases with aspect ratio, impacting overall storage efficiency.
    - Required base gas volume increased by 2,700, 48, and 18 percent between aspect ratios 1 and 12 for the Fixed Diameter model set, Fixed Volume and Casing Shoe Depth model set, and Fixed Volume and Cavern Mid-Height model set, respectively.
- **Working Gas Capacity:** In the Fixed Diameter model set, working gas capacity increases with aspect ratio due to larger cavern volume.
    - Working gas capacity increased by 1,200 percent between aspect ratios 1 and 12.
      In the Fixed Volume model sets, working gas capacity decreases with aspect ratio as a result of stress-related volume loss at deeper depths.
    - Working gas capacity decreased by 15 and 26 percent for the Fixed Volume and Casing Shoe Depth model set and Fixed Volume and Cavern Mid-Height model set, respectively.
      The Fixed Volume and Cavern Mid-Height model set had the highest overall working gas capacity due to deeper casing shoe depths enabling higher pressure conditions.
- **Storage Efficiency:** Storage efficiency declines with increasing aspect ratio due to rising base gas requirements.
    - Storage efficiency decreased by 18, 12, and 11 percent between aspect ratios 1 and 12 for the Fixed Diameter model set, Fixed Volume and Casing Shoe Depth model set, and Fixed Volume and Cavern Mid-Height model set, respectively.
      The Fixed Diameter model set showed the most significant efficiency loss due to volume increase with aspect ratio.
- **Casing Strain:** Casing strain is more influenced by roof diameter than aspect ratio.
    - Minimal change in casing strain was observed across the Fixed Diameter model set.
      In the Fixed Volume model sets, lower aspect ratios (larger roof diameters) resulted in higher casing strain.
    - Casing strain is predicted to be 93 and 87 percent lower at an aspect ratio of 12 compared to an aspect ratio of 1 within the Fixed Volume and Casing Shoe Depth model set and Fixed Volume and Cavern Mid-Height model set, respectively.
      Strain was most pronounced in the Fixed Volume and Cavern Mid-Height model set due to deeper depths and associated thermal and stress conditions.

Overall, low aspect ratio caverns offer advantages in storage efficiency due to reduced base gas requirements, while high aspect ratio caverns with smaller roof diameters help minimize casing strain. However, these benefits come with trade-offs: low aspect ratio designs tend to require larger roof spans, which can increase casing strain, whereas high aspect ratio designs are more susceptible to closure and require higher minimum pressures due to their greater depth.

Optimal cavern design balances maximizing working gas capacity, minimizing base gas requirements, while maintaining cavern stability. This balance is further influenced by surface facility constraints, well spacing requirements, and operational considerations such as pressure cycling and long-term cavern integrity. Cavern operators should consider these interdependencies holistically to tailor cavern geometry to site-specific geological and operational conditions.

References

Callahan, G. D., A. F. Fossum, and D. K. Svalstad, 1989. *Documentation of SPECTROM-32: A Finite Element Thermomechanical Stress Analysis Program*, DOE/CH/10378-2, prepared by RE/SPEC Inc., Rapid City, SD, for the U.S. Department of Energy, Chicago Operations Office, Argonne, IL, Vols. I and II.

Munson, D. E., 1998. *Analysis of Multistage and Other Creep Data for Domal Salts*, SAND98-2276, Sandia National Laboratories, Albuquerque, NM.

Nieland, J. D., 2004. *Salt Cavern Thermal Simulator Version 2.0 User's Manual*, RSI-1760, prepared by RESPEC, Rapid City, SD, for the Gas Technology Institute, Des Plaines, IL.

Osnes, J.D., K. L. DeVries, J. L., Ratigan, M. W. Meece, M. Thomson, and G. W. Spencer, 2007. "A Case History of the Threaded Coupling Production Casing Failure in Gas Caverns – Part 1: Detection and Geomechanical Analysis," *Solution Mining Research Institute Fall Meeting,* Halifax, Nova Scotia, October 7–10, pp. 41–69.

Vining, C. A. and K. L. DeVries, 2011. *Geomechanical Design Study of Natural Gas Storage in Well GH-001 in the Arcadia Salt Dome, Louisiana*, RSI-2201, prepared by RESPEC, Rapid City, SD, for PB Energy Storage Services, Inc., Houston, TX (draft).

Van Sambeek, L.L., J.L. Ratigan, and F.D. Hansen. 1993. "Dilatancy of Rock Salt in Laboratory Tests." *Proceedings of the 34th U.S. Symposium on Rock Mechanics*, University of Wisconsin–Madison, Madison, WI, 30, B. C. Haimson (ed.), International Journal of Rock Mechanics and Mining Sciences & Geomechanics Abstracts, Pergamon Press, Vol. 30, No. 7, pp. 735–738.